MJFAS MALAYSIAN JOURNAL OF FUNDAMENTAL AND APPLIED SCIENCES
PRINT ISSN: 2289-5981 | ONLINE ISSN: 2289-599X

RESEARCH ARTICLE

# *Artocarpus integer* peel as a highly effective low-cost adsorbent for methylene blue removal: Kinetics, isotherm, thermodynamic and pelletized studies

Rosalyza Hasan [a], Nurul Adina Mohamed Razifuddin [a], Nurfatehah Wahyuny Che Jusoh [b], Rohayu Jusoh [a], Herma Dina Setiabudi [a, c, *]

[a] *Faculty of Chemical & Natural Resources Engineering, Universiti Malaysia Pahang, 26300 Gambang, Pahang, Malaysia*
[b] *Department of Environmental Engineering and Green Technology, Malaysia-Japan International Institute of Technology, Universiti Teknologi Malaysia KL Campus, Jalan Sultan Yahya Petra, 54100, Kuala Lumpur, Malaysia*
[c] *Centre of Excellence for Advanced Research in Fluid Flow, Universiti Malaysia Pahang, 26300 Gambang, Kuantan, Pahang, Malaysia*

* *Corresponding author: herma@ump.edu.my*

**Article history**
Submitted 5 October 2017
Revised 27 November 2017
Accepted 2 January 2018
Published 8 March 2018

**Graphical abstract**

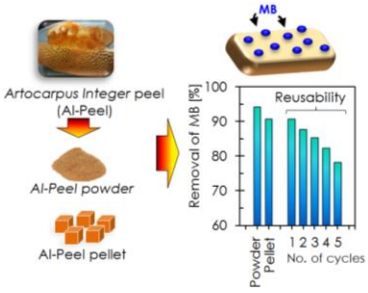


**Abstract**

Recently, there is a growing interest in identifying low-cost alternative adsorbents which have reasonable adsorption efficiency for dye removal. In this study, agricultural waste, *Artocarpus Integer* peel (AI-Peel) was used as the adsorbent to remove methylene blue (MB) from aqueous solution. The batch adsorption process was conducted to evaluate the effect of contact time (1 – 40 min), adsorbent dosage (0.25 – 4.0 g $L^{-1}$), pH (2 – 8), initial dye concentration (100 – 500 mg $L^{-1}$) and temperature (30 – 50 $^{o}$C). The experimental data followed well pseudo-second-order kinetic model and Langmuir isotherm (Type 2) with maximum adsorption capacity of 396.825 mg $g^{-1}$. The analysis of thermodynamic studies indicated that the adsorption process was exothermic, controlled by a chemisorption process, feasible and spontaneous in nature with decrease in degree of spontaneity at higher temperature. The characterization results revealed that the functional groups of AI-Peel play an important role in the adsorption of MB onto AI-Peel. The study of pelletized and reusability of AI-Peel indicated the great potential of pelletized AI-Peel as low-cost adsorbent for efficient removal of MB from aqueous solution. This study successfully discovers a new highly effective low-cost adsorbent for MB removal.

***Keywords*:** Low-cost adsorbent, agricultural waste, *Artocarpus Integer* peel, pelletized adsorbent, methylene blue



## INTRODUCTION

Dyes have been extensively used in many industries, such as textile, leather, paper production and plastic manufacturer. The fast development of these industries has contributed to an increase in the concentration of dyes in wastewater. The discharged of this wastewater into water body became significant sources of pollution due to their undesirable colour which will reduce sunlight penetration and resist photochemical and biological attacks to aquatic life. Besides, these dyes are toxic as well as carcinogenic, mutagenic, and teratogenic, that could affect aquatic life and also humans. Hence, it is utmost crucial to remove dyes from wastewater to ensure safe discharge of this effluent into the water body. Several techniques have been extensively developed and used to remove dyes in wastewater such as membrane filtration [1-2], photocatalysis [3-4], coagulation-flocculation [5] and adsorption [6-1]. However, adsorption has been identified to be more effective method, which could overcome the shortcomings associated with cost, complexity and time consuming.

Among various adsorbents developed and used to adsorb dyes, activated carbon is one of the most widely used. However, the high demand for activated carbons in other advanced applications such as catalyst supports, air filters and gas storage, resulted in increasing their cost. Therefore, there is a growing interest in identifying low-cost alternative adsorbents which have reasonable adsorption efficiency including agricultural solid wastes [9-11], industrial solid wastes [12,13] and natural materials [14,15]. However, most of these adsorbents still have limited adsorption capacities and low removal percentage of dyes as compared to the activated carbon.

Artocarpus integer is a species of tree in the family of Moraceae, and in the same genus as breadfruit (Artocarpus altilis) and jackfruit (Artocarpus heterophyllus L.), which can be found in Southeast Asia. With the increase in the production of processed fruit product, abundant amount of Artocarpus integer peels (AI-Peel) are disposed from food processing sector, causing a serious problem of disposal. Thus, utilizing of AI-Peel as an alternative low-cost adsorbent would increase the economic value, help to reduce the cost of disposal and consequently can reduce the environmental pollution.

Based on the above mentioned considerations, in this study, the use of the AI-Peel as low-cost adsorbent for the removal of methylene blue (MB) from aqueous solution was reported. The adsorption process was investigated as the function of contact time, adsorbent dosage, pH, initial dye concentration and temperature. The characteristics of the adsorption isotherm, kinetics and thermodynamics were also studied through the adsorption process. For industrial purpose, the usage of palletized adsorbent is highly recommended due to its easy handling process and also recyclable feature. Therefore, in this study, the

efficiency and feasibility of pelletized AI-Peel for efficient process were also investigated.

## EXPERIMENTAL

### Chemicals

Methylene Blue (MB) was purchased from Merck (Sdn Bhd, Malaysia) with C.I. 52015, chemical formula of $C_{16}H_{18}N_3SCl$ and molecular weight of 319.85 g $mol^{-1}$. The maximum wavelength of MB is 668 nm.

### Preparation of the adsorbent

The *Artocarpus Integer* peel (AI-Peel) was collected from the local area at Pahang, Malaysia. The AI-Peel was cut to obtain a size range of 10 – 20 mm. The pieces were soaked in distilled water overnight to remove the surface adhering impurities, followed with oven-dried at 80 ºC for 24 hours. The dried pieces were then ground and sieved to 355-600 µm particles sizes, followed with oven-dried at 100 ºC overnight until the weight was constant before being stored in a plastic bottle.

### Characterization

The infrared spectra of the AI-Peel before and after adsorption were obtained using Fourier-transform infrared (FTIR) (Perkin Elmer Spectrum GX FTIR Spectroscopy). The sample were prepared as KBR pallets and scanned over the range of 4000 – 400 $cm^{-1}$ to identify the functional group of AI-Peel that might be involved in the adsorption process. The specific surface area and pore volume of AI-Peel were measured using Thermo-Scientific Surfer.

### Adsorption studies

The MB stock solution was prepared by dissolving accurately the measured amounts of MB in deionized water to obtain a concentration of 1000 mg $L^{-1}$, before being diluted to desired concentration (100 – 500 mg $L^{-1}$). The pH of working solutions was adjusted to the desired value with sodium hydroxide, NaOH (Merck) and hydrochloric acid, HCl (Merck). Adsorption experiments were performed in a batch-adsorption system.

In brief, specific amounts of AI-Peel (0.25 – 4.0 g $L^{-1}$) were added in a 250 ml conical flask containing 200 ml of MB solution. The mixtures were stirred at 300 rpm at temperature range of 30 – 50 ºC. Then, the samples were withdrawn at appropriate time intervals and centrifuged at 3500 rpm. The residuals of the MB concentration were determined by using the UV/vis spectrophotometer at 668 nm. The amounts of adsorption at time $t$, $q_t$ (mg $g^{-1}$) was calculated by the following equation,

$$\text{Adsorption capacity}, q_t\ (\text{mg g}^{-1}) = \left(\frac{C_o - C_t}{W}\right) \times V \qquad (1)$$

where, $C_o$ (mg $L^{-1}$) and $C_t$ (mg $L^{-1}$) are the concentration of MB at initial and at any time $t$, respectively. $V$ (L) is the volume of the dye solution and $W$ (g) is the mass of the adsorbent used.

The MB removal percentage can be calculated as follows,

$$\text{Removal}\ (\%) = \left(\frac{C_o - C_t}{C_o}\right) \times 100 \qquad (2)$$

where, $C_o$ (mg $L^{-1}$) and $C_t$ (mg $L^{-1}$) are the concentration of MB at initial and at any time $t$, respectively.

All of the experiments were carried out triplicate to ensure the accuracy of the experimental data.

### Preparation of the palletized AI-Peel

In order to study the efficiency of pelletized AI-Peel towards adsorption of MB, 0.4 g of AI-Peel powder was pelletized using hot press at 80 ºC and 15 MPa for 30 min of hold time to obtain palletized AI-Peel with volume of 0.512 $cm^3$. Three different sizes (L × W × H) of palletized AI-Peel were used in this study; (i) 0.8 cm × 0.8 cm × 0.8 cm, (ii) 1.0 cm × 0.64 cm × 0.8 cm, and (iii) 1.5 cm × 0.43 cm × 0.8 cm.

## RESULTS AND DISCUSSION

### Effect of contact time

The effect of contact time in the range of 1 to 40 minutes were studied at initial dye concentration of 100 mg $L^{-1}$, adsorbent dosage of 1 g $L^{-1}$, pH solution of 6, and a temperature of 30 °C. The percentage removal of MB as a function of contact time is shown in Fig. 1. The percentage MB removal was increased with the increasing in contact time until it reached optimum at 20 min. Beyond 20 min, there was no increase in MB removal and a steady-state approximation was assumed. The contact time curve shows that the MB removal was rapid in the first 12 min. The curves of contact time are single, smooth and continuous leading to saturation indicating the possible monolayer coverage of dye on the surface of AI-Peel. This result is in agreement with the study reported by Kallel et al. for the adsorption of MB onto garlic straw [7].

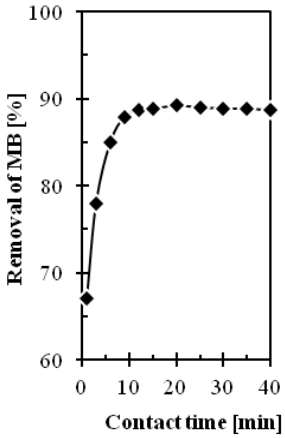


**Fig. 1** Effect of contact time on the adsorption of MB dye onto AI-Peel ($C_o$ = 100 mg $L^{-1}$, $W$ = 1 g $L^{-1}$, pH 6, $T$ = 30 ºC).

### Effect of adsorbent dosage

In order to investigate the effect of adsorbent dosage (AI-Peel) on MB adsorption, experiments were conducted at initial dye concentration of 100 mg $L^{-1}$, pH solution of 6 and a temperature of 30 °C, while the amount of adsorbent added was varied.

Fig. 2 shows a plot of the MB removal under various absorbent dosages ranging from 0.25 to 4.0 g $L^{-1}$. At equilibrium time, the percentage MB removal increased with an increase in AI-Peel dosage up to 2 g $L^{-1}$ and thereafter remained unchanged with further increase in adsorbent dosage. The increase in percentage MB removal was due to the increase in the available sorption surface and sites with adsorbent dosage. A similar trend was observed for the removal of MB onto wheat straw [8], garlic straw [7] and rejected tea [16].

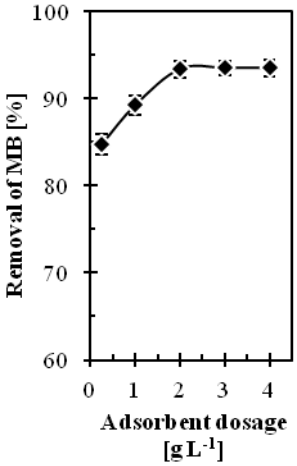


**Fig. 2** Effect of adsorbent dosage on the adsorption of MB dye onto AI-Peel ($C_o$ = 100 mg $L^{-1}$, pH 6, $T$ = 30 ºC, $t$ = 20 min).

### Effect of pH

The pH value of the dye solution has been recognized as an important factor in adsorption process, which influences the surface charge and the dissociation of functional groups on active sites [17]. In this study, the effects of pH of MB solution were examined over a pH range of 2 – 8, and the results are illustrated in Fig. 3A. It could be observed that the MB removal was increased with the increasing of pH up to 6, and then nearly constant over the pH ranges of 6 – 8. This behavior could be described on the basis of zero point charge ($pH_{zpc}$) of the AI-Peel adsorbent, which determined to be at ~ pH 3.9 (Fig. 3B). At pH less than the $pH_{zpc}$, the adsorbent surface is positively changed, thus making the $H^+$ ions effectively competed with the MB cations, which caused the lower MB removal. Whereas, at pH higher than the $pH_{zpc}$, the surface of AI-Peel became negatively charged, thus allowing the electrostatic attraction of positively charged MB cations (in water, MB readily dissociates into $MB^+$ and $Cl^-$) [18]. Similar trend was observed for adsorption of methylene blue onto almond gum [11], peach shell [17] and citrus limetta peel [19].

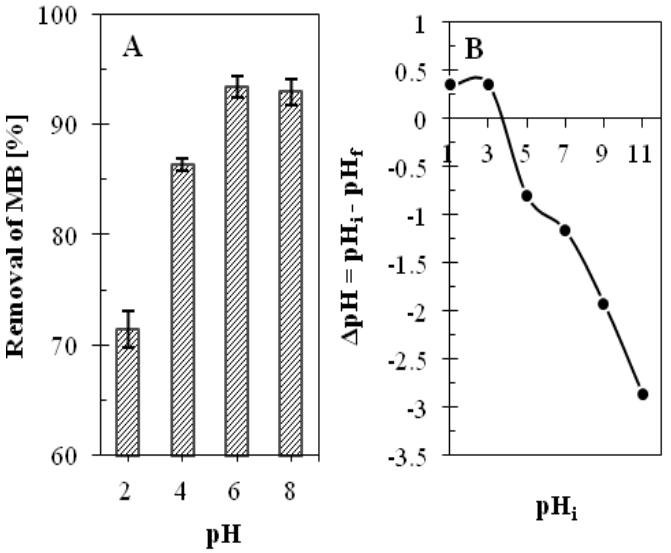


**Fig. 3** (A) Effect of pH on the adsorption of MB dye onto AI-Peel ($C_o$ = 100 mg $L^{-1}$, $W$ = 2 g $L^{-1}$, $T$ = 30 ºC, $t$ = 20 min). (B) $pH_{zpc}$ of AI-Peel adsorbent.

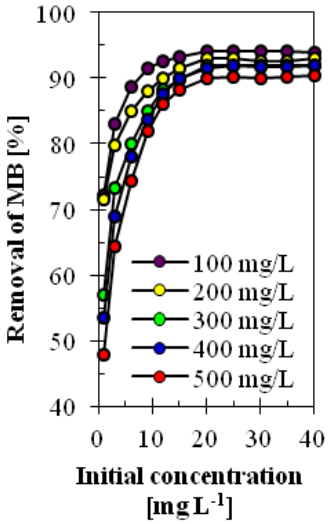


**Fig. 4** Effect of initial concentration on the adsorption of MB dye onto AI-Peel ($W$ = 2 g $L^{-1}$, pH 6, $T$ = 30 ºC).

### Effect of initial concentration

The effect of the initial MB concentration on the percentage removal of MB is given in Fig. 4. It was found that more than 80% of the MB was removed in the first 10 minutes of adsorption and increased slowly to maximum at equilibrium. As shown in Fig. 4, there are three main stages during the adsorption process which are the movement of the MB molecules from the bulk solution to the external surface of the AI-Peel (film diffusion), the movement of the MB molecules to the interior regions of the AI-Peel (particle diffusion) and the sorption of the MB on the interior surfaces of the pores of AI-Peel (sorption) [6]. This process takes longer time at higher MB concentration that might be due to the agglomeration of MB molecules at high concentration, which may slow down the adsorption process. Similar phenomenon was observed on the adsorption of MB onto cocoa pod husk [20].

### Adsorption Isotherm Studies

The analysis of the adsorption isotherm model is a prerequisite for predicting the adsorption uptake of the adsorbent, which is one of the main parameters required for designing an optimized adsorption system. For this purpose, the adsorption kinetic isotherm studies were conducted at AI-Peel dosage of 2 g $L^{-1}$, initial pH of 6, temperature of 30 ºC, and contact time of 20 minutes with different initial concentration of 100 – 500 mg $L^{-1}$.

The equilibrium data for MB adsorption onto AI-Peel were modelled with the Langmuir (four linearized expression) [21], Freundlich [22], Temkin [23], and Dubinin-Radushkevich [24] models were used for this purpose. The linearized forms of these four isotherm models are presented as follows:

Langmuir isotherm (Type 1):

$$\frac{C_e}{q_e} = \frac{1}{q_m K_L} + \frac{C_e}{q_m} \tag{3}$$

Langmuir isotherm (Type 2):

$$\frac{1}{q_e} = \left(\frac{1}{q_m K_L}\right)\left(\frac{1}{C_e}\right) + \frac{1}{q_m} \tag{4}$$

Langmuir isotherm (Type 3):

$$q_e = q_m - \left(\frac{1}{K_L}\right)\frac{q_e}{C_e} \tag{5}$$

Langmuir isotherm (Type 4):

$$\frac{q_e}{C_e} = K_L q_m - K_L q_e \tag{6}$$

Freundlich isotherm:

$$\log q_e = \log K_f + \frac{1}{n}\log C_e \tag{7}$$

Temkin isotherm:

$$q_e = B \ln A + B \ln C_e \tag{8}$$

Dubinin-Radushkevich isotherm:

$$\ln q_e = \ln q_m - K_{DR}\varepsilon^2 \tag{9}$$

where $C_e$ is the MB concentration at equilibrium (mg $L^{-1}$), $q_e$ is the adsorption capacity at equilibrium (mg $g^{-1}$), $q_m$ is the maximum adsorption capacity (mg $g^{-1}$), $K_L$ is the Langmuir constant (L $mg^{-1}$), $K_f$ is the Freundlich equilibrium constant ((mg $g^{-1}$)(L $mg^{-1})^{1/n}$)), $n$ is an empirical constant, $B$ is the Temkin constant, $A$ is the Temkin equilibrium binding constant (L $g^{-1}$), $K_{DR}$ is Dubinin-Radushkevich constant ($mol^2$ $kJ^{-2}$) and $\varepsilon$ is the Polanyi potential (J $mol^{-1}$), in which can be calculated from $\varepsilon = RT \ln (1+1/C_e)$.

**Table 1** Isotherm parameters for adsorption of MB onto AI-Peel.

| Isotherm | Parameters | Value |
|---|---|---|
| Langmuir (Type 1) | $q_m$ (mg g$^{-1}$) | 476.191 |
| | $K_L$ (L mg$^{-1}$) | 0.018 |
| | $R^2$ | 0.986 |
| Langmuir (Type 2) | $q_m$ (mg g$^{-1}$) | 396.825 |
| | $K_L$ (L mg$^{-1}$) | 0.019 |
| | $R^2$ | 0.999 |
| Langmuir (Type 3) | $q_m$ (mg g$^{-1}$) | 451.360 |
| | $K_L$ (L mg$^{-1}$) | 0.019 |
| | $R^2$ | 0.968 |
| Langmuir (Type 4) | $q_m$ (mg g$^{-1}$) | 461.355 |
| | $K_L$ (L mg$^{-1}$) | 0.019 |
| | $R^2$ | 0.968 |
| Freundlich | n | 1.349 |
| | $K_f$ (mg g$^{-1}$)(L mg$^{-1}$)$^{1/n}$ | 12.885 |
| | $R^2$ | 0.998 |
| Temkin | $B$ (J mol$^{-1}$) | 83.019 |
| | $A$ (L g$^{-1}$) | 0.258 |
| | $R^2$ | 0.965 |
| Dubinin-Radushkevich | $q_m$ (mg g$^{-1}$) | 171.330 |
| | $K_{DR}$ (×10$^5$) (mol$^2$ kJ$^{-2}$) | 1 |
| | $R^2$ | 0.844 |

**Table 2** Comparison of the maximum adsorption capacities of various adsorbents for MB removal.

| Adsorbent | Adsorption capacity (mg g$^{-1}$) | Ref |
|---|---|---|
| Artocarpus Integer peel | 396.825 | This work |
| Citrus grandis peel | 344.83 | [25] |
| Jackfruit peel | 285.71 | [26] |
| Cocoa pod husk | 263.90 | [20] |
| Garlic straw | 256.41 | [7] |
| Almond gum | 250.00 | [11] |
| Broad bean peel | 192.70 | [27] |
| Peach shells | 183.60 | [17] |
| Rejected tea | 147.00 | [16] |
| Garlic peel | 82.64 | [26] |
| Activated carbon prepared from bamboo | 454.20 | [19] |
| Activated carbon prepared from date stone | 316.11 | [28] |
| Activated carbon prepared from oil palm fiber | 312.50 | [29] |

The values of isotherm parameters are listed in Table 1. To quantitatively compare the accuracy of the models, the correlation coefficients ($R^2$) were also calculated and are also listed in Table 1. Analysis of the $R^2$ values suggests that Langmuir isotherm (Type 2) model better described the adsorption of MB onto AI-Peel, which indicates that the adsorption of MB onto AI-Peel takes place as monolayer adsorption on a surface that is homogeneous in adsorption affinity. The monolayer adsorption process was also observed on the adsorption of MB onto various low cost adsorbents including pomelo (*Citrus grandis*) peel [25], wheat straw [8], garlic peel [26] and broad bean peel [27]. According to Table 1, the Langmuir $q_m$ value was 396.825 mg g$^{-1}$, and $K_L$ constant was 0.019. The $R_L$ value [$R_L = 1/(1+K_L C_o)$] for the system, which demonstrates the favourability of the adsorption system was calculated to be 0.094, indicating the favourable adsorption of MB onto AI-Peel because of the value falls between 0 and 1 [26].

Table 2 lists a comparison of maximum monolayer adsorption capacity of MB on various adsorbents. It can be seen that the AI-Peel is more effective for the adsorption of MB even when being compared with some of the activated carbon reported in the literature, indicating the great potential of AI-Peel as alternative adsorbent for MB removal.

## Adsorption Kinetics

Adsorption kinetics is essential for understanding the adsorbate uptake rate and the mechanism of the process. The adsorption kinetic studies were conducted at AI-Peel dosage of 2 g L$^{-1}$, initial pH of 6, temperature of 30 $^o$C, and contact time of 20 minutes with different initial concentration of 100 – 500 mg L$^{-1}$. In this study, the equilibrium data for MB adsorption onto AI-Peel were modelled with the pseudo-first-order [30], pseudo-second-order [31] and intraparticle diffusion [32] models. The linearized forms of these models were represented as follow:

Pseudo-first-order equation:

$$\ln (q_e - q_t) = \ln q_e - k_1 t \tag{10}$$

Pseudo-second-order equation:

$$\frac{t}{q_t} = \frac{1}{k_2 q_e^2} + \frac{1}{q_e} t \tag{11}$$

Intraparticle diffusion equation:

$$q_t = k_{id} t^{1/2} + C \tag{12}$$

where $q_e$ is the adsorption capacity at equilibrium (mg g$^{-1}$), $q_t$ is the adsorption capacity at any time $t$ (mg g$^{-1}$), $k_1$ and $k_2$ are the adsorption constant of pseudo-first-order and pseudo-second-order model and $K_{id}$ is the intraparticle diffusion rate constant (mg g$^{-1}$ min$^{-1/2}$).

The linear regression coefficient, $R^2$ and parameters of pseudo-first-order and pseudo-second-order kinetic models are listed in Table 3. The conformity between experimental data and the model predicted values are expressed by the correlation coefficients ($R^2$) and the $q_e$ values. Based on the results reported in Table 3, the highest value of $R^2$ was observed with the pseudo-second-order model ($R^2 \geq 0.999$) for all concentrations. Additionally, the strong agreement between $q_e$ values obtained from pseudo-second-order model and the experimental values confirmed the suitability of this model in fitting the kinetic data. This observation indicated that the adsorption rate is more likely controlled by the chemisorption process and that the rate of reaction is directly proportional to the number of active sites on the surface of the adsorbent [7]. Similar results were also presented for adsorption of MB onto pomelo (*Citrus grandis*) peel [25], wheat straw [8], garlic peel [26] and broad bean peel [27].

**Table 3** Kinetic parameters for adsorption of MB onto AI-Peel

| Models | Parameters | 100 mg L$^{-1}$ | 200 mg L$^{-1}$ | 300 mg L$^{-1}$ | 400 mg L$^{-1}$ | 500 mg L$^{-1}$ |
|---|---|---|---|---|---|---|
| **Experimental** | $q_{e,exp}$ (mg g$^{-1}$) | 47.050 | 93.000 | 137.965 | 183.800 | 225.000 |
| **Pseudo-first-order** | $q_e$ (mg g$^{-1}$) | 10.486 | 24.666 | 56.885 | 92.790 | 134.210 |
| | $k_1$ (min$^{-1}$) | 0.2054 | 0.182 | 0.191 | 0.203 | 0.220 |
| | $R^2$ | 0.948 | 0.995 | 0.994 | 0.995 | 0.997 |
| **Pseudo-second-order** | $q_e$ (mg g$^{-1}$) | 47.847 | 95.238 | 142.860 | 192.310 | 238.100 |
| | $k_2$ (min$^{-1}$) | 0.050 | 0.019 | 0.007 | 0.005 | 0.003 |
| | $R^2$ | 0.999 | 0.999 | 0.999 | 0.999 | 0.999 |

To identify the possible step in controlling the adsorption of MB onto AI-Peel under the selected conditions, the experimental data was then fitted the intraparticle diffusion equation. It can be seen in Fig. 5 that the plot did not pass through the origin and were not linear over the entire time range, which implies that intraparticle diffusion was not the sole rate-limiting step. At lower initial MB concentration, a rapid increase in the uptake rate to the maximum adsorption capacities at equilibrium was observed indicating that the uptake of MB ions by the AI-Peel was very fast. Meanwhile, at higher initial MB concentration, the adsorption process take place through several steps due to the molecular collusions of MB molecules which hindered the movement of MB ions towards the surface of AI-Peel. In brief, the adsorption of MB onto AI-Peel involved the movement of the MB molecules from the bulk solution to the external surface of the AI-Peel (film diffusion), the movement of the MB molecules to the interior regions of the AI-Peel (particle diffusion) and the sorption of the MB molecules on the interior surfaces of the pores of AI-Peel (sorption).

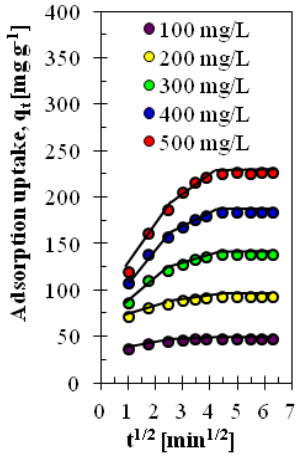


**Fig. 5** Intraparticle diffusion plot for adsorption of MB dye onto AI-Peel ($W$ = 2 g L$^{-1}$, pH 6, $T$ = 30 ºC).

The parameters of intraparticle diffusion model are given in Table 4. It was observed that the values of the intercept $C$ increased with an increase in initial MB concentration which indicated an increasing boundary layer effect as the initial MB concentration increased [6]. A similar behaviour was reported for the adsorption of MB onto wheat straw [8].

**Table 4** Intraparticle diffusion model constant and correlation coefficients for adsorption of MB onto AI-Peel.

| Initial MB concentration (mg L$^{-1}$) | Intraparticle diffusion model | | |
|---|---|---|---|
| | C | $k_{id}$ (mg g$^{-1}$ min$^{-1/2}$) | $R^2$ |
| 100 | 41.694 | 1.238 | 0.885 |
| 200 | 75.675 | 3.999 | 0.973 |
| 300 | 99.996 | 8.819 | 0.953 |
| 400 | 124.770 | 13.809 | 0.949 |
| 500 | 144.56 | 19.041 | 0.910 |

## Thermodynamics Studies

Thermodynamics parameters were evaluated to investigate the nature of the adsorption process. The effect of temperature on the removal of MB onto AI-Peel was studied at AI-Peel dosage of 2 g L$^{-1}$, initial pH of 6, initial concentration of 100 mg L$^{-1}$, and contact time of 20 minutes over temperature range of 30 – 50 ºC. The thermodynamic parameters, including the free Gibbs energy (ΔGº), enthalpy (ΔHº) and entrophy (ΔSº) were calculated using the following equations [6]:

$$\ln K_C = \frac{\Delta S^O}{R} - \frac{\Delta H^O}{RT} \quad (13)$$

$$K_c = \frac{C_e\,(\text{adsorbent})}{C_e\,(\text{solution})} \quad (14)$$

$$\Delta G^O = -RT \ln K_C \quad (15)$$

where $K_c$ is the equilibrium constant of the adsorption, $R$ is the universal gas constant (8.314 J mol$^{-1}$ K$^{-1}$) and $T$ is the absolute solution temperature (K). The values of $\Delta H^o$ and $\Delta S^o$ were obtained from the slope and intercept of the plot of $K_c$ versus 1/$T$, respectively. The values of $\Delta H^o$, $\Delta S^o$ and $\Delta G^o$ are listed in Table 5.

**Table 5** Thermodynamic parameters for the adsorption of MB onto AI-Peel.

| $E_a$ (kJ mol$^{-1}$) | $\Delta H^o$ (kJ mol$^{-1}$) | $\Delta S^o$ (kJ mol$^{-1}$ K$^{-1}$) | $\Delta G^o$ (kJ mol$^{-1}$) | | | | |
|---|---|---|---|---|---|---|---|
| | | | 30 ºC | 35 ºC | 40 ºC | 45 ºC | 50 ºC |
| 41.528 | -44.947 | -0.133 | -4.727 | -4.063 | -3.399 | -2.735 | -2.072 |

The negative value of $\Delta H^o$ (-44.947 kJ mol$^{-1}$) and $\Delta S^o$ (-0.133 kJ mol$^{-1}$ K$^{-1}$) indicated that the adsorption process was exothermic with a decrease in the randomness at solid-liquid interface with increasing temperature. A negative sign with a decrease in magnitude of $\Delta G^o$ with an increase in temperature indicates that the process is feasible and spontaneous in nature with decrease in degree of spontaneity at higher temperature. A similar result was reported in the literature for the adsorption of crystal violet onto activated sintering process red mud [33].

The value of the activation energy ($E_a$) can be obtained by the Arrhenius equation,

$$\ln k_2 = \ln A - \frac{E_a}{R}\left(\frac{1}{T}\right) \quad (16)$$

where $k_2$ is a pseudo-second-order rate constant of adsorption (g/mg·min), $R$ is the universal gas constant (8.314 J mol$^{-1}$ K$^{-1}$) and $T$ is the absolute solution temperature (K). The slope of the plot ln $k_2$ versus 1/$T$ resulted in a value for the $E_a$ that was 41.528 kJ mol$^{-1}$ (Table 5) indicating a chemisorption process.

## Characterization of AI-Peel

The FTIR analysis was performed to identify the possible functional groups in AI-Peel that may be involved in the adsorption process. Fig. 6 shows the FTIR spectra of AI-Peel before and after adsorption of MB. The FTIR spectra of AI-Peel samples indicate the presence of various functional groups at wavelengths 3414 cm$^{-1}$ (O–H stretching) [9,17], 2938 cm$^{-1}$ (C–H stretching) [9], 1747 cm$^{-1}$ (C=O stretching) [17], 1630 cm$^{-1}$ (N–H bending) [10], 1430 cm$^{-1}$ (C-H deformation in lignin) [7], 1070 cm$^{-1}$ (C–O stretching) [9,17] and 655 cm$^{-1}$ (C–H deformation in cellulose) [17]. The interaction of MB molecules with functional groups of AI-Peel was confirmed by the reduction of several peaks significantly at 3414, 2938, 1747, 1630, 1430 and 1070 cm$^{-1}$ indicating that the main functional groups that contributed to adsorption were O–H, C–H, C=O, N–H and C–O. In brief, the presence of functional groups on the surface of AI-Peel provides considerable interaction with MB molecules during the adsorption process. The reduction in the several peaks of FTIR after the adsorption of MB was also reported in the adsorption of MB onto garlic straw [7].

The presence of MB molecules on the surface of AI-Peel was also confirmed by the reduction in the BET surface area and average of pore

diameter of AI-Peel after the adsorption process. The BET surface area and average of pore diameter of AI-Peel before adsorption was 0.9270 $m^2 g^{-1}$ and 0.6717 nm, respectively, while after adsorption was 0.7072 $m^2 g^{-1}$ and 0.4107 nm, respectively.

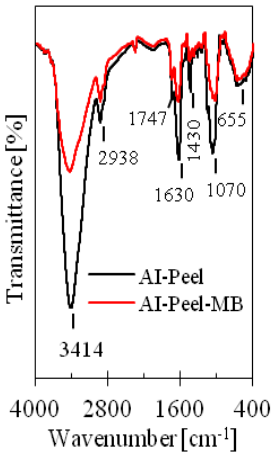


**Fig. 6** FTIR spectra of the AI-Peel before and after MB adsorption.

### Pelletized and reusability studies

For the industrial purpose, the application of adsorbent in the form of pellet is more applicable as compared to the powder form, in which pellet is easy to handle and recycle. Therefore, in this study, the pelletized AI-Peel was prepared with three different shapes as shown in Table 6 with the fixed amount of adsorbent (0.4 g) for each pellet. The adsorption process were conducted at initial MB concentration of 100 mg $L^{-1}$, adsorbent dosage of 2 g $L^{-1}$, pH solution of 6 and a temperature of 30 °C. As observed in Table 6, the removal percentage of MB using all size of pelletized AI-Peel was greater than 85% indicating the great potential of pelletized AI-Peel for industrial application. In addition, it is noted that the different shape of pellet did not significantly affected the performance of adsorbent.

**Table 6** AI-Peel pellet specification and removal percentage of MB.

| Pellet Size | Dimension | Removal of MB [%] |
|---|---|---|
| 0.8 cm × 0.8 cm × 0.8 cm |  | 90.66 |
| 1.0 cm × 0.64 cm × 0.8 cm |  | 87.42 |
| 1.5 cm × 0.43 cm × 0.8 cm |  | 85.13 |

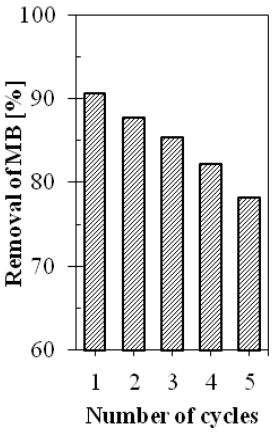


**Fig. 7** Reusability of pelletized AI-Peel for MB removal.

The feasibility of using pelletized AI-Peel to remove MB from aqueous solution was further studied with the multiple adsorption cycles. Pelletized AI-Peel with size of 0.8 cm × 0.8 cm × 0.8 cm was used in this study. In brief, the pelletized AI-Peel was oven-dried at 80 °C overnight after every adsorption cycle to evaluate its reusable ability. As observed in Fig. 7, there is only small decreased (12.56%) in the removal percentage of MB after 5 cycles indicating the good performance of pelletized AI-Peel during multiple adsorption cycles.

## CONCLUSION

The present study demonstrated that the agricultural solid waste, *Artocarpus integer* peel (AI-Peel) can be used as an effective adsorbent for the removal of MB from aqueous solution. The results indicated that the experimental data were fitted well to Langmuir isotherm (Type 2) with maximum adsorption capacity of 396.825 mg $g^{-1}$. The kinetics of MB adsorption onto AI-Peel was followed pseudo-second-order kinetic model. Thermodynamic studies indicated that the adsorption process was exothermic, controlled by a chemisorption process, feasible and spontaneous in nature with decrease in degree of spontaneity at higher temperature. The study of palletized AI-Peel found that the removal percentage of MB using all size of pelletized AI-Peel was greater than 85% indicating the great potential of pelletized AI-Peel for further used in a fixed bed column study. Moreover, the reusability study confirmed the feasibility of pelletized AI-Peel for multiple cycles of adsorption.

## ACKNOWLEDGEMENT

The authors would like to express their deep gratitude to Universiti Malaysia Pahang (UMP) for providing the laboratory facilities and financial support through RDU170331.

## REFERENCES

[1] Wang, J., Qin, L., Lin, J., Zhu, J., Zhang, Y., Liu, J., and Van der Bruggen, B. 2017. Enzymatic construction of antibacterial ultrathin membranes for dyes removal. *Chemical Engineering Journal*. 323: 56–63.

[2] Liu, M., Chen, Q., Lu, K., Huang, W., Lü, Z., Zhou, C., Yu, S., and Gao, C. 2017. High efficient removal of dyes from aqueous solution through nanofiltration using diethanolamine-modified polyamide thin-film composite membrane. *Separation and Purification Technology*. 173: 135–143.

[3] Mohite, S. V., Ganbavle, V. V., and Rajpure, K. Y. 2017. Photoelectrocatalytic activity of immobilized Yb doped $WO_3$ photocatalyst for degradation of methyl orange dye. *Journal of Energy Chemistry*. *26*(3): 440–447.

[4] May-Lozano, M., Mendoza-Escamilla, V., Rojas-García, E., López-Medina, R., Rivadeneyra-Romero, G., and Martinez-Delgadillo, S. A. 2017. Sonophotocatalytic degradation of Orange II dye using low cost photocatalyst. *Journal of Cleaner Production*. *148*: 836–844.

[5] Issa Hamoud, H., Finqueneisel, G., and Azambre, B. 2017. Removal of binary dyes mixtures with opposite and similar charges by adsorption, coagulation/flocculation and catalytic oxidation in the presence of $CeO_2/H_2O_2$ Fenton-like system. *Journal of Environmental Management*. *195*: 195–207.

[6] Jalil, A. A., Triwahyono, S., Yaakob, M. R., Azmi, Z. Z. A., Sapawe, N., Kamarudin, H. N., Setiabudi, H. D., Jaafar, N. F., Sidik, S. M., Adam, S. H., and Hameed, B. H. 2012. Utilization of bivalve shell-treated *Zea mays L.* (maize) husk leaf as a low-cost biosorbent for enhanced adsorption of malachite green. *Bioresource Technology*. 120: 218-224.

[7] Kallel, F., Chaari, F., Bouaziz, F., Bettaieb, F., Ghorbel, R., and S. E. Chaabouni, S. E. 2016. Sorption and desorption characteristics for the removal of a toxic dye, methylene blue from aqueous solution by a low cost agricultural by-product. *Journal of Molecular Liquids*. 219: 279-288.

[8] Lin, Q., Wang, K., Gao, M., Bai, Y., Chen, L., and Ma, H. 2017. Effectively removal of cationic and anionic dyes by pH-sensitive amphoteric adsorbent derived from agricultural waste-wheat straw. *Journal of the Taiwan Institute of Chemical Engineers*. *76*: 65–72.

[9] Kristanti, R. A., Kamisan, M. K. A., and Hadibarata, T. 2016. Treatability of methylene blue solution by adsorption process using *Neobalanocarpus hepmii* and *Capsicum annuum*. *Water, Air, and Soil Pollution*. 227(5): 134-141.

[10] Rahmat, N. A., Ali, A. A., Salmiati, Hussain, N., Muhamad, M. S., Kristanti, R. A., and Hadibarata, T. 2016. Removal of remazol brilliant

blue R from aqueous solution by adsorption using pineapple leaf powder and lime peel powder. *Water, Air, and Soil Pollution*. 227(4): 105-115.

[11] Bouaziz, F., Koubaa, M., Kallel, F., Chaari, F., Driss, D., Ghorbel, R. E., and Chaabouni, S. E. 2015. Efficiency of almond gum as low-cost adsorbent for methylene blue dye removal from aqueous solutions. *Industrial Crops and Products*. 74: 903-911.

[12] Ferrero, F. 2015. Dye removal from aqueous solution using coal fly ash for continuous flow adsorption. *Clean technologies and Enivironmental Policy*. 17(7): 1907-1915.

[13] Dağdelen, S., Acemioğlu, B., Baran, E., and Koçer, O. 2014. Removal of remazol brilliant blue R from aqueous solution by pirina pretreated with nitric acid and commercial activated carbon. *Water, Air and Soil Pollution*. 225(3): 1899-1913.

[14] Wang, W., Wang, F., Kang, Y., and Wang, A. 2015. Enhanced adsorptive removal of methylene blue from aqueous solution by alkali-activated palygorskite. *Water, Air, and Soil Pollution*. 226(3): 83-95.

[15] Berez, A., Schäfer, G., Ayari, F., and Trabelsi-Ayadi, M. 2016. Adsorptive removal of azo dyes from aqueous solutions by natural bentonite under static and dynamic flow conditions. *International Journal of Enviornmental Science and Technology*. 13(7): 1625-1640.

[16] Nasuha, N., Hameed, B. H., and Din, A. T. M. 2010. Rejected tea as a potential low-cost adsorbent for the removal of methylene blue. *Journal of Hazardous Materials*. 175(1-3): 126-132.

[17] Marković, S., Stanković, A., Lopičić, Z., Lazarević, S., Stojanović, M., and Uskoković, D. 2015. Application of raw peach shell particles for removal of methylene blue. *Journal of Environmental Chemical Engineering*. 3(2): 716-724.

[18] Momčilović, M., Purenović, M., Miljković, M., Bojić, A., and Ranđelović, M. 2011 . Adsorption of cationic dye methylene blue onto activated carbon obtained from horse chestnut kernel. *Hemijska Industrija*. 65: 123-129.

[19] Shakoor, S. and Nasar, A. 2016. Removal of methylene blue dye from artificially contaminated water using citrus limetta peel waste as a very low cost adsorbent. *Journal of the Taiwan Institute of Chemical Engineers*. *66*: 154–163.

[20] Pua, F. L., Sajab, M. S., Chia, C. H., Zakaria, S., Rahman, I. A., and Salit, M. S. 2013. Alkaline-treated cocoa pod husk as adsorbent for removing methylene blue from aqueous solutions. *Journal of Environmental Chemistry Engineering*. 1(3): 460-465.

[21] Langmuir, I. 1918. The adsorption of gases on plane surfaces of the glass, mica nad platinum. *Journal of the American Chemical Society*. 40(9): 1361-1403.

[22] Freundlich, H. M. F. 1906. Over the Adsorption in Solution. *The Journal of Physical Chemistry A*. 57: 385-470.

[23] Temkin, M. J. and Pyzhev, V. 1940. Recent Modifications to Langmuir Isotherms. *Acta Physicochim.* URSS 12: 217-222.

[24] Misra, D. N., 1969. Adsorption on heterogeneous surfaces: A dubinin-radushkevich equation. *Surface Science*. 18(2): 367-372.

[25] Hameed, B. H., Mahmoud, D. K., and Ahmad, A. L. 2008. Sorption of dye from aquesous solution by pomelo (*Citrus grandis*) peel in a batch system. *Colloids and Surfaces A: Physicohemical and Engineering Aspects*. 316(1-3): 78-84.

[26] Hameed, B. H., and Ahmad, A. A. 2009. Batch adsorption of methylene blue from aqueous solution by garlic peel, an agricultural waste biomass. *Journal of Hazardous Materials*. 164(2-3): 870-875.

[27] Hameed, B. H., and El-Khaiary, M. I. 2008. Sorption kinetics and isotherm studies of a cationic dye using agricultural waste: Broad bean peels. *Journal of Hazardous Materials*. 154(1-3): 639-648.

[28] Foo, K. Y., and Hameed, B. H. 2011. Preparation of activated carbon from date stones by microwave induced chemical activation: Application for methylene blue adsorption. *Chemical Engineering Journal*. 170(1): 338-341.

[29] Foo, K. Y., and Hameed, B. H. 2011. Microwave-assisted preparation of oil palm fiber activated carbon for methylene blue adsorption. *Chemical Engineering Journal*. 166(2): 792-795.

[30] Lagergren, S. 1898. About the theory of so-called adsorption of soluble substances. *Kungliga Svenska Vetenskapsakademiens Handlingar*. 24(4): 1-39.

[31] Ho, Y. S., and McKay, G. 1999. Pseudo-second order model for sorption processes. *Process Biochemistry*. 34(5): 451-465.

[32] Weber, W. J., and Morris, J. C. 1963. Kinetics of adsorption on carbon from solution. *Journal of the Sanitary Engineering Division*. 89(2): 31-59.

[33] Zhang, L., Zhang, H., Guo W., and Tian, Y. 2014. Removal of malachite green and crystal violet cationic dyes from aqueous solution using activated sintering process red mud. *Applied Clay Science*. 93–94: 85-93.